Science Signaling
AAAS

www.sciencesignaling.org/cgi/content/full/3/119/ra32/DC1

Supplementary Materials for

SUMOylation of the Transcriptional Co-Repressor KAP1 Is Regulated by the Serine and Threonine Phosphatase PP1

Xu Li, H. Helen Lin, Hanqing Chen, Xingzhi Xu, Hsiu-Ming Shih, David K. Ann*

*To whom correspondence should be addressed. E-mail: dann@coh.org

Published 27 April 2010, *Sci. Signal.* **3**, ra32 (2010)
DOI: 10.1126/scisignal.2000781

The PDF file includes:

Methods

Cell culture

Cells were maintained at 37°C in 5% CO_2 as follows: HEK 293 cells were cultured in Dulbecco's modified Eagle's medium (DMEM) supplemented with 10% fetal bovine serum FBS), penicillin (50 U/ml), and streptomycin (50 μg/ml); MCF-7 cells were cultured in DMEM, 10% FBS with recombinant human insulin (0.01 mg/ml); MCF-7/TR/sh-KAP1 cells were cultured in MCF-7 medium containing blasticidin (10 μg/ml) and zeocin (100 μg/ml); and MCF-7/sh-KAP1, MCF-7/sh-PP1α, MCF-7/sh-PP1β, MCF-7/sh-I-2, and MCF-7/sh-Control cell lines were cultured in MCF-7 medium containing puromycin (2 μg/ml).

Western blotting analysis

Whole-cell lysates were prepared by lysing cells with RIPA buffer [25 mM tris-HCl (pH 8.0), 125 mM NaCl, 1% Nonidet-P-40, 0.5% sodium deoxycholate, 0.1% sodium dodecyl sulfate (SDS), 0.004% sodium azide, 10 mM N-ethylmaleimide (NEM), 1 mM NaF, 2 mM Na_3VO_4, and a Complete Protease Inhibitor Cocktail (Roche)], and were subjected to SDS-polyacrylamide gel electrophoresis (SDS-PAGE), followed by Western blotting analysis with antibodies against FLAG-KAP1 (M2, Sigma-Aldrich), HA (COVANCE), tubulin (D-10), and enhanced green fluorescent protein (EGFP), ATM pSer^{1981} (Santa Cruz Biotechnology), KAP1 pSer^{824}, PP1α, PP1β, PP1γ (all from BETHYL). Dilution of antibodies prior to use was performed according to the manufacturers' instructions. Western blots were visualized with an enhanced chemiluminescence detection kit (ECL-Plus, Amersham Pharmacia Biotech) and a Versadoc 5000 Imaging System (Bio-Rad). Densitometric tracing data were obtained and analyzed with Quantity One Software (Bio-Rad). The results of Western blotting analyses shown in the figures are representative of 2 to 4 independent experiments.

Production of lentiviruses and transduction of cells

pLKO.1 lentiviral vectors harboring shRNAs specific for human KAP1, PP1α, PP1β, or I-2 or a random sequence (as a control) (sh-KAP1, sh-PP1α, sh-PP1β, sh-I-2, and sh-Control, respectively), pΔ8.7, and pVSV-G were used for lentiviral production in HEK 293FT cells as previously described (*1*). For transduction with lentiviruses, HEK 293 or MCF-7 cells were plated 1 day prior to infection and were cultured overnight to reach ~70% confluence. The culture medium was then aspirated and fresh medium containing the concentrated lentiviruses of interest was added and incubated for 24 hours in the presence of polybrene (8 μg/ml). The transduced cells were selected and maintained in HEK 293 or MCF-7 medium with puromycin (2 μg/ml) and pools of stable cells were used in the studies reported herein.

Luciferase assays

MCF-7/TR/sh-KAP1 cells were cotransfected with the *p21*-Luc reporter (*2*) and a firefly control reporter, pRL-TK (for normalization) with Lipofectamine 2000 (Invitrogen). Luciferase assays were performed with DualGlo Luciferase Assay Kit (Promega). The desired luciferase activity was calculated by normalization against the firefly luciferase activity.

In vitro SUMOylation Assays

In vitro SUMOylation assays were performed by cotransfecting HEK 293 cells with plasmids encoding FLAG-tagged KAP1 or its mutants and EGFP-SUMO-1 in a 1:4 ratio, together with HA-PP1α or HA-PP1β with Lipofactamine 2000. SUMOylated KAP1 was detected by Western

blotting analysis of whole-cell lysates with antibodies against the FLAG tag and EGFP.

Immunoprecipitations

Whole-cell lysates were prepared by lysing cells with RIPA buffer containing an additional 10 mM NEM, 1 mM NaF, 2 mM Na_3VO_4 and a Complete Protease Inhibitor Cocktail. Antibodies against KAP1, PP1α, PP1β, or PP1γ (5 μg/ml) were mixed with 1 mg of whole-cell lysate and samples were rotated at 4°C for 2 hours. Protein A/G PLUS-Agarose (Santa Cruz Biotechnology) was then added, and samples were rotated at 4°C overnight, washed with three times with 1 ml of 1X PBS, and immunoprecipitates were eluted in 40 μl of 2X SDS sample buffer. Samples were subjected to Western blotting analysis with the appropriate antibodies. Alternatively, HEK 293 cells or MCF-7 cells were cotransfected with plasmids encoding FLAG-tagged KAP1 or its mutants together with plasmids encoding HA-PP1α, HA-PP1β, or HA-PP2cA with Lipofactamine 2000 and were then processed after 24 hours as described above, with antibodies against the appropriate tag.

Isolation of total RNA and real-time reverse transcription PCR

Total RNA from control and doxorubicin-treated MCF-7 cells was extracted with TRIzol reagent (Invitrogen), treated with RNAase-free DNAase (Invitrogen), and re-extracted with phenol-chloroform, followed by ethanol precipitation. Reverse transcription and quantitative PCR of *p21*, *Bax*, *Puma* and *Noxa* mRNAs were performed with the iTaq SYBR Green Supermix (BioRad), a fraction of each sample of total RNA, and specific pairs of gene-specific primers (table S1). PCR amplification and fluorescence detection were performed with the MyIQ real-time PCR detection system, and threshold cycles were determined by the iCycler program (in default setting). Fold differences were determined with the ΔΔCt method with 18*S* ribosomal RNA (rRNA) as a control.

Cell cycle analysis

To analyze DNA content, harvested cells were centrifuged at 1,000*g* for 5 min, washed with PBS, fixed in 70% ethanol, treated with RNase (10 μg/ml for 30 min at 37°C), washed with PBS, and stained (for 30 min) with 0.5 ml of propidium iodide (PI, 69 μmol/l) or DAPI (50 μmol/l) in sodium citrate (38 μmol/l). Cell cycle phase distribution was determined by analytic DNA flow cytometry, as described by Keyomarsi *et al*. (*3*). The percentage of cells in each phase of the cell cycle was analyzed with Summit, Modfit, and Flowjo software. For Annexin-V analysis, Annexin-V-FITC (0.5 μg/ml, BD Phamingen) and DAPI (0.05 μg/ml) were used for each sample.

Statistical analysis

Statistical analyses were performed with one-way ANOVA, followed by posthoc comparisons based on modified Newman-Keuls-Student procedure with $P < 0.05$ considered significant. Where appropriate, unpaired Student's *t*-tests were also performed to determine differences between two data groups. Error bars in the figures represent the SD of the mean.

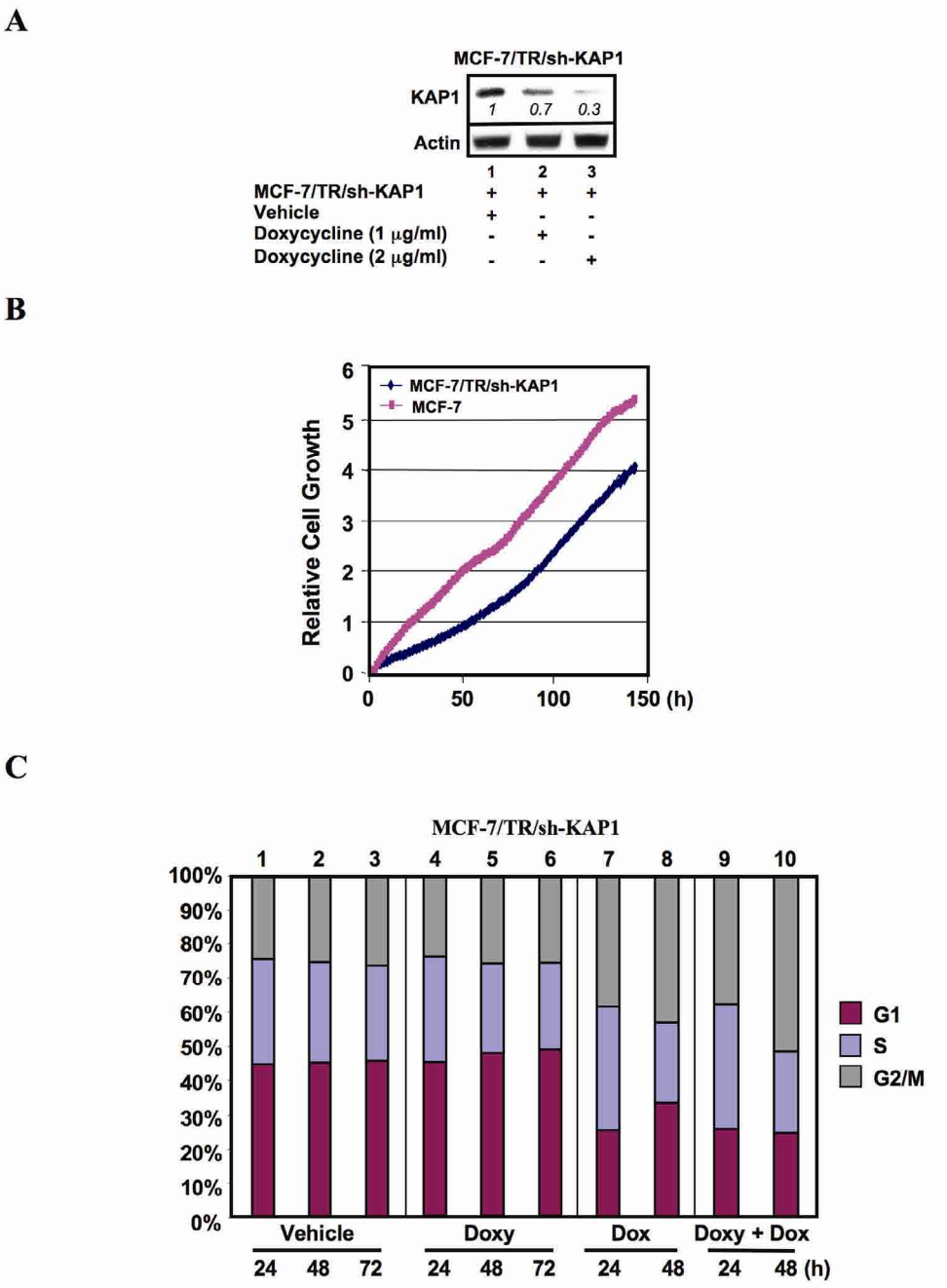

Fig. S1. Tetracycline-inducible knockdown of KAP1 decreases the proliferation of MCF-7 cells. (**A**) The abundance of KAP1 protein diminished in MCF-7/TR/sh-KAP1 cells upon induction of the expression of KAP1-specific shRNA by treatment with doxycycline (1 μg/ml or 2 μg/ml) for 48 hours. Relative amounts (in italics) of steady-state KAP1 protein normalized to those of actin are shown. (**B**) Proliferation rates of MCF-7 cells and KAP1-depleted MCF-7/TR/sh-KAP1 cells were compared with the Real-time Cell Growth Monitoring system. (**C**) Unsynchronized MCF-7/TR/sh-KAP1 cells were treated with a combination of doxycycline (Doxy, 2 μg/ml) and doxorubicin (Dox, 1 μM) for the indicated time periods. KAP1-depleted MCF-7/TR/sh-KAP1 cells were increasingly arrested at the G_2/M-phase of the cell cycle at 24 and 48 hours after treatment with doxorubicin.

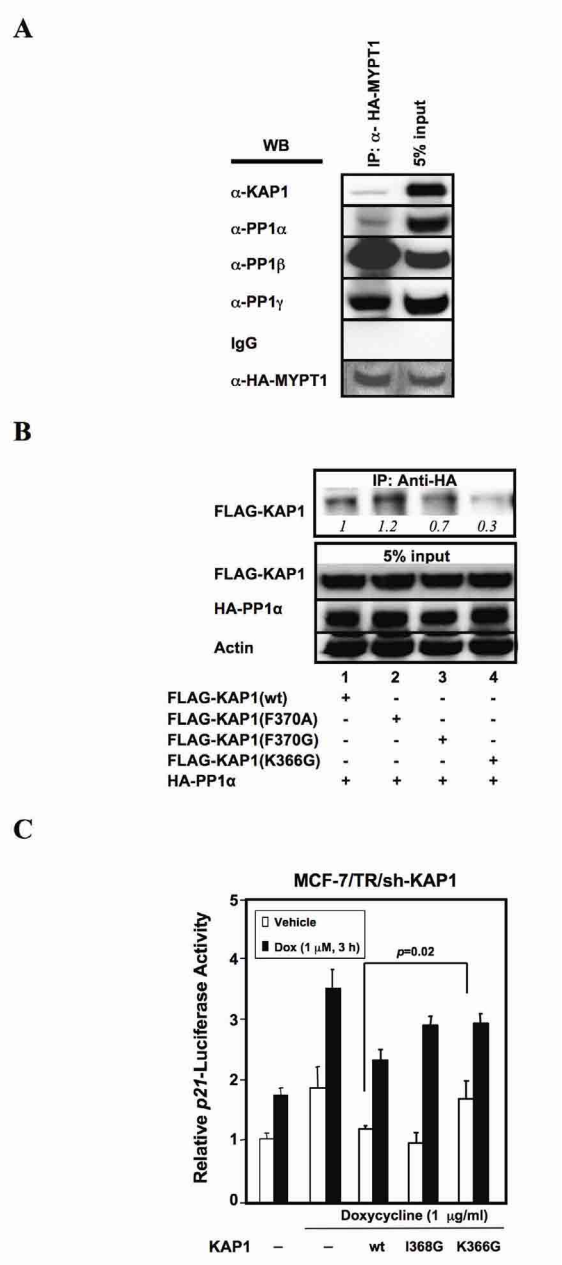

Fig. S2. The F370A and F370G mutations have opposing effects on the interactions of KAP1 with PP1α. (**A**) Whole-cell extracts prepared from HEK 293 cells transfected with plasmid encoding HA-MYPT1were subjected to coimmunoprecipitation experiments with an antibody against HA and were visualized as described for Fig. 2A. (**B***)* HEK 293 cells were cotransfected with plasmids encoding HA-PP1α and FLAG-tagged KAP1 or its mutants, as indicated. An antibody against HA was used in the immunoprecipitations and coimmunoprecipitated KAP1 (WT or KAP1 mutants) were visualized with an antibody against FLAG. Relative binding (numbers in italics) of KAP1 (WT or mutant proteins) with PP1α, after normalization, is shown, and the binding of KAP1(wt) to PP1α was set to 1. (**C**) MCF-7/TR/sh-KAP1 cells were transiently transfected with *p21*-Luc and plasmids encoding WT or mutant KAP1 proteins. After treatment with vehicle or doxycycline (1 μg/ml), transfected cells were treated as described for Fig. 2D and the luciferase activity of *p21*-Luc was measured and normalized against that of the firefly control reporter (pRL-TK). Results represent the mean ± SD from 6 independent experiments). $P < 0.05$ was considered significant.

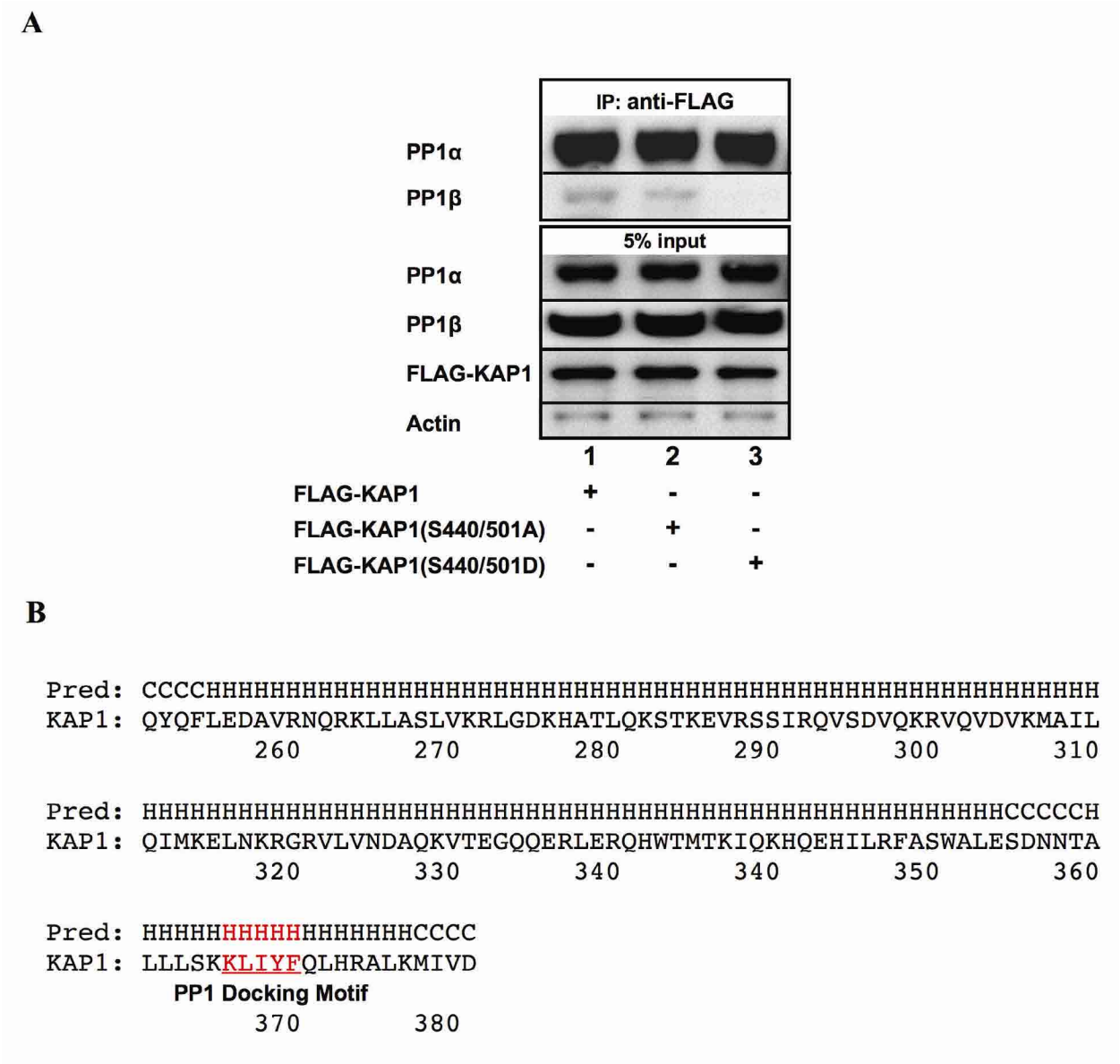

Fig. S3. The S440/501A and S440/501D double mutations of KAP1 do not affect its interaction with PP1α or PP1β or the predicted secondary structure of the PP1-docking motif. (**A**) Whole-cell extracts prepared from HEK 293 cells transfected with plasmids encoding FLAG-KAP1(S440/S501A) or FLAG-KAP1(S440/S501D) were subjected to immunoprecipitation with an antibody against FLAG, and coimmunoprecipitated PP1α or PP1β were visualized as described for Fig. 2A. (**B**) The predicted secondary structure of the KAP1 PP1-docking motif (366KLIYF370), based on the PSIPRED secondary protein structure prediction method (*4*), is shown. H, α-helix; C, coiled-coil.

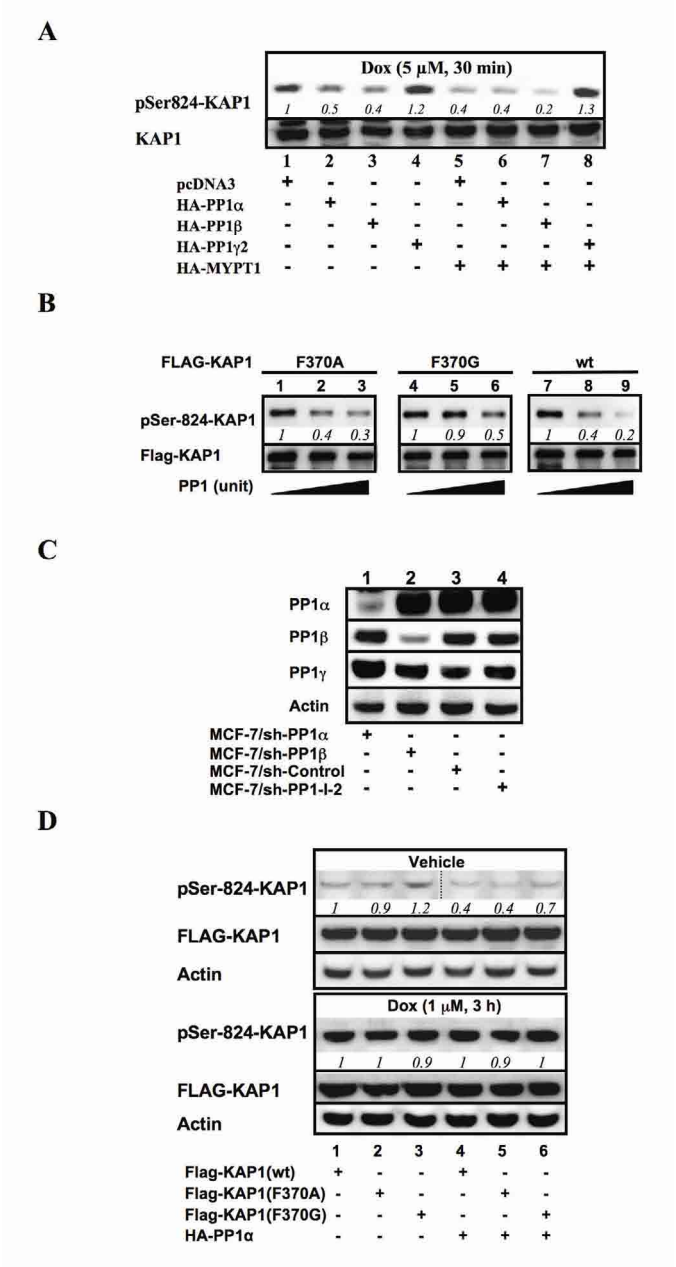

Fig. S4. The F370G mutation of KAP1 attenuates the PP1α-dependent dephosphorylation of pSer^{824}. (**A**) The effect of the increased abundance of PP1α, PP1β and PP1γ2, in the absence and presence of exogenous MYPT1, on doxorubicin-induced phosphorylation of Ser^{824} of endogenous KAP1. Relative amounts (numbers in italics) of KAP1 pSer^{824} normalized against that of total KAP1 are shown. (**B**) In vitro phosphatase assays were performed with increasing amounts of purified rabbit skeletal muscle PP1 and pSer^{824}-containing FLAG-KAP1(wt), FLAG-KAP1(F370G), or FLAG-KAP1(F370A). (**C**) Efficient knockdown of PP1α and PP1β in MCF-7 cells was achieved by lentivirus-based, specific shRNAs. The amounts of PP1α, PP1β, PP1γ and actin in pooled cells is shown to confirm the specificity of each shRNA. (**D**) MCF-7 cells were transfected with plasmids encoding FLAG-tagged KAP1 or its mutants as well as HA-PP1α and were treated as indicated. The phosphorylation profile of KAP1 Ser^{824} was analyzed by Western blotting (n = 3 independent experiments). The relative abundance of pSer^{824} (numbers in italics) of the various KAP1 proteins, after normalization, is shown.

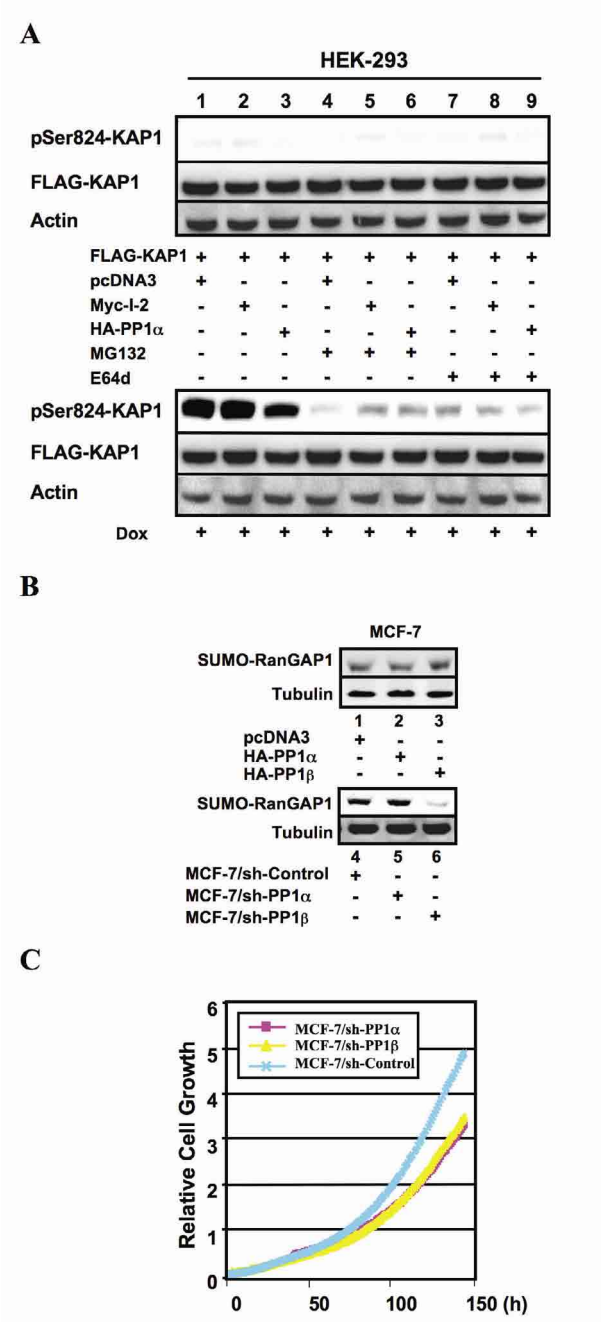

Fig. S5. PP1α and PP1β and the regulation of KAP1 Ser^{824} phosphorylation, RanGAP1 SUMOylation, and MCF-7 cell proliferation. (**A**) HEK 293 cells were transiently transfected with empty vector or with plasmids encoding HA-PP1α or Myc-I-2. After 24 hours recovery, cells were pretreated for 1 hour with vehicle, MG132 (5 μM), or E64d (10 μM), and then treated for 30 min with vehicle or doxorubicin (5 μM). Protein extracts were analyzed by Western blotting with antibodies against KAP1, KAP1 pSer^{824}, and actin. (**B**) Endogenous SUMOylation of RanGAP1 was assessed by Western blotting of extracts of cells transfected with plasmids encoding PP1α or PP1β (*upper panel*) or in cells in which PP1α and PP1β had been knocked down (*lower panel*) (n = 3 experiments). (**C**) Growth rates of MCF-7/sh-PP1α, MCF-7/sh-PP1β, and MCF-7/sh-Control cells were compared with the Real-time Cell Growth Monitoring system.

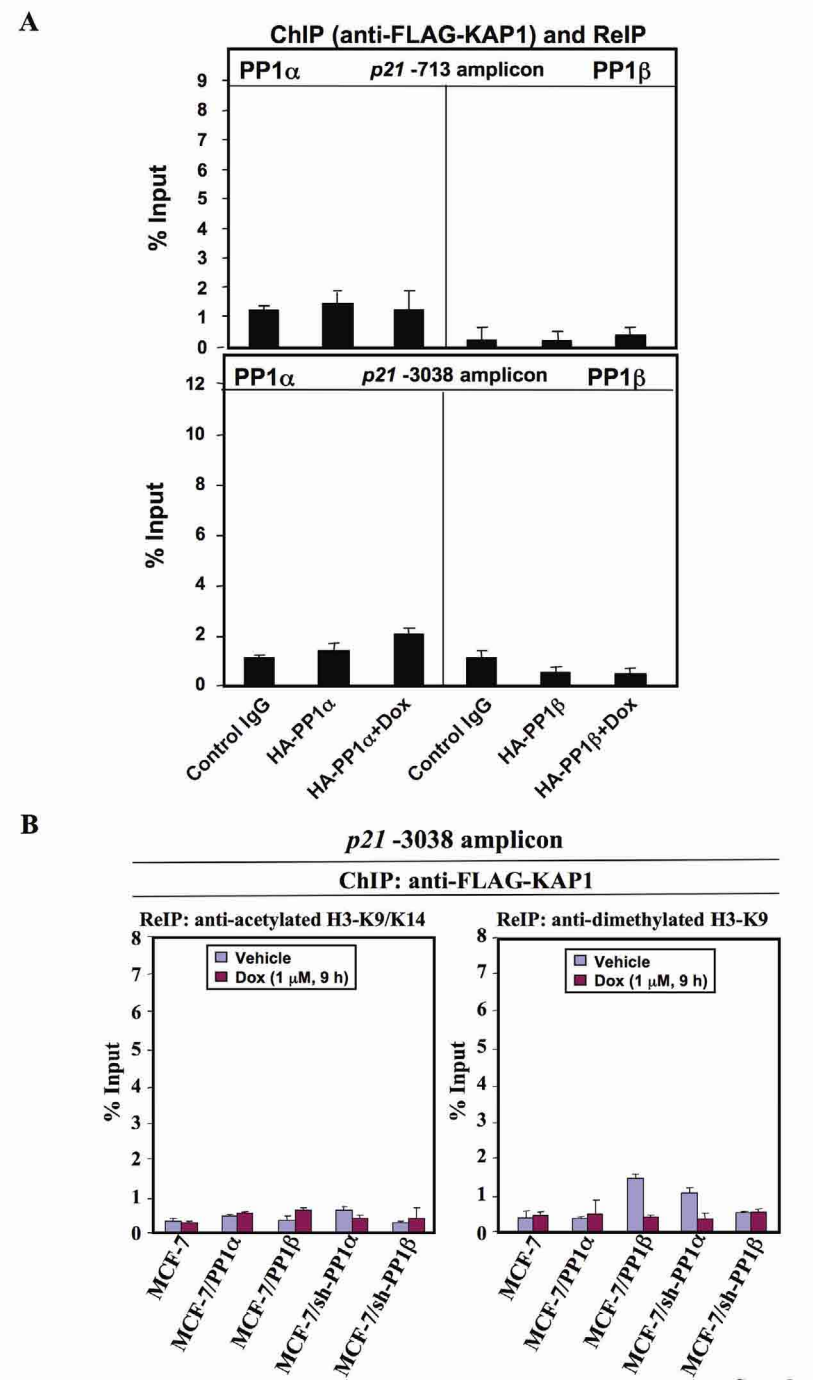

Fig. S6. PP1α and PP1β do not occupy the -713 and -3038 distal regions of *p21* and they fail to affect the modification of K9 in histone H3 at the -3038 distal region. (**A**) ChIP-ReIP experiments were performed as described for Fig. 6A. Quantification was performed by real-time PCR with primer pairs against the -3038 and -713 amplicons of endogenous *p21* (table S1). (**B**) ChIP-ReIP experiments were performed as described for Fig. 6B. Quantification was performed by real-time PCR with primer pairs against the -3038 amplicon of endogenous *p21* (table S1). Results represent the mean ± SD of 3 independent experiments. $P < 0.05$ was considered significant.

Table S1. Primer pairs used in real-time PCR assays. FP, forward primer; RP, reverse primer.

Primer	Purpose	Sequence (5' to 3')
18S rRNA FP	Real-time RT-PCR	CGGCGACGACCCATTCGAAC
18S rRNA RP	Real-time RT-PCR	GAATCGAACCCTGATTCCCCGTC
p21 FP	Real-time RT-PCR	TTTCTCTCGGCTCCCCATGT
p21 RP	Real-time RT-PCR	GCTGTATATTCAGCATTGTGGG
Bax FP	Real-time RT-PCR	CCGATTCATCTACCCTGCTG
Bax RP	Real-time RT-PCR	CAATTCCAGAGGCAGTGGAG
Noxa FP	Real-time RT-PCR	ATTACCGCTGGCCTACTGTG
Noxa RP	Real-time RT-PCR	GTGCTGAGTTGGCACTGAAA
Puma FP	Real-time RT-PCR	CTGTGAATCCTGTGCTCTGC
Puma RP	Real-time RT-PCR	AATGAATGCCAGTGGTCACA
p21 -20 amplicon FP	ChIP (real-time PCR)	TATATCAGGGCCGCGCTG
p21 -20 amplicon RP	ChIP (real-time PCR)	CTTCGGCAGCTGCTCACACCT
p21 -713 amplicon FP	ChIP (real-time PCR)	TTTCCCTGGAGATCAGGTTG
p21 -713 amplicon RP	ChIP (real-time PCR)	GGAAGGAGGGAATTGGAGAG
p21 -3038 amplicon FP	ChIP (real-time PCR)	CAGGCTGGTCTCAAAACTCC
p21 -3038 amplicon RP	ChIP (real-time PCR)	GCCTGTAATCCCAGCACTTT

References

1. H. V. Nguyen, J. L. Chen, J. Zhong, K. J. Kim, E. D. Crandall, Z. Borok, Y. Chen, D. K. Ann, SUMOylation attenuates sensitivity toward hypoxia- or desferroxamine-induced injury by modulating adaptive responses in salivary epithelial cells. *The American journal of pathology* **168**, 1452–1463 (2006).

2. Y. K. Lee, S. N. Thomas, A. J. Yang, D. K. Ann, Doxorubicin down-regulates Kruppel-associated box domain-associated protein 1 sumoylation that relieves its transcription repression on p21WAF1/CIP1 in breast cancer MCF-7 cells. *J. Biol. Chem.* **282**, 1595–1606 (2007).

3. K. Keyomarsi, D. Conte, Jr., W. Toyofuku, M. P. Fox, Deregulation of cyclin E in breast cancer. *Oncogene* **11**, 941–950 (1995).

4. L. J. McGuffin, K. Bryson, D. T. Jones, The PSIPRED protein structure prediction server. *Bioinformatics* **16**, 404–405 (2000).